

# Clinical Mapping Approach to Diagnose Electrical Rotors and Focal Impulse Sources for Human Atrial Fibrillation

SANJIV M. NARAYAN, M.Sc., M.D., Ph.D.,\* DAVID E. KRUMMEN, M.D.,\*  
and WOUTER-JAN RAPPEL, Ph.D.†

From the \*Veterans' Affairs and University of California Medical Centers, San Diego, California, USA; and †Institute for Theoretical Biological Physics, University of California, San Diego, California, USA

[Correction added after online publication 26-Apr-2012: Figure 5 has been updated.]

**Computational Mapping of Rotors and Focal Impulses in Human AF.** *Introduction:* The perpetuating mechanisms for human atrial fibrillation (AF) remain undefined. Localized rotors and focal beat sources may sustain AF in elegant animal models, but there has been no direct evidence for localized sources in human AF using traditional methods. We developed a clinical computational mapping approach, guided by human atrial tissue physiology, to reveal sources of human AF.

*Methods and Results:* In 49 AF patients referred for ablation ( $62 \pm 9$  years; 30 persistent), we defined repolarization dynamics using monophasic action potentials (MAPs) and recorded AF activation from 64-pole basket catheters in left atrium and, in  $n = 20$  patients, in both atria. Careful positioning of basket catheters was required for optimal mapping. AF electrograms at 64–128 electrodes were combined with repolarization and conduction dynamics to construct spatiotemporal AF maps. We observed sustained sources in 47/49 patients, in the form of electrical rotors ( $n = 57$ ) and focal beats ( $n = 11$ ) that controlled local atrial activation with peripheral wavebreak (fibrillatory conduction). Patients with persistent AF had more sources than those with paroxysmal AF ( $2.1 \pm 1.0$  vs  $1.5 \pm 0.8$ ,  $P = 0.02$ ), related to shorter cycle length ( $163 \pm 19$  milliseconds vs  $187 \pm 25$  milliseconds,  $P < 0.001$ ). Approximately one-quarter of sources lay in the right atrium.

*Conclusions:* Physiologically guided computational mapping revealed sustained electrical rotors and repetitive focal beats during human AF for the first time. These localized sources were present in 96% of AF patients, and controlled AF activity. These results provide novel mechanistic insights into human AF and lay the foundation for mechanistically tailored approaches to AF ablation. (*J Cardiovasc Electrophysiol*, Vol. 23, pp. 447-454, May 2012)

*atrial fibrillation, catheter ablation, fibrillatory conduction, mapping, rotors*

## Introduction

Despite great strides in percutaneous and surgical therapy for atrial fibrillation (AF),<sup>1-3</sup> their efficacy remains suboptimal.<sup>2,4</sup> Seminal observations by Haïssaguerre<sup>1</sup> revealed that ectopic beats from the pulmonary veins (PVs) may trigger AF, establishing AF ablation therapy with PV isolation as its cornerstone.<sup>1,2</sup> However, the mechanisms that perpetuate

AF once it has been triggered are not defined.<sup>5,6</sup> Historically, detailed mapping defined the patient-specific sustaining mechanisms that now serve as ablation targets for the routine cure of supraventricular or ventricular arrhythmias,<sup>7</sup> yet the complex and highly variable cycle-to-cycle activation of AF makes traditional mapping difficult.

We hypothesized that a novel approach to mapping AF, that physiologically interprets fibrillatory wave activity by analyzing widely sampled simultaneous multisite electrograms in the context of rate-dependent atrial repolarization and conduction, may enable identification of AF-sustaining mechanisms. There are 2 prevailing hypotheses. The multiwavelet hypothesis proposes that continuously meandering electrical waves cause AF.<sup>8,9</sup> However, this hypothesis does not readily explain consistent spatial nonuniformities in AF,<sup>10,11</sup> while ablation designed to address this hypothesis rarely terminates AF and has modest success.<sup>2,12</sup> Alternatively, the localized source hypothesis is based on experimental models in which reentrant circuits (rotors)<sup>6,13,14</sup> or focal impulses<sup>11,15</sup> activate rapidly enough to cause disorganized AF. However, there has until now been no<sup>9</sup> or little<sup>16,17</sup> evidence to support localized sources in human AF.

We tested our hypothesis by developing a computational mapping approach, employing careful wide-area mapping of the atria during AF and analysis of tissue conduction and repolarization, to create individualized spatiotemporal maps of AF in patients with paroxysmal and persistent AF referred for percutaneous ablation.

This manuscript was processed by a guest editor.

This work was supported by grants to Dr. Narayan from the NIH (HL70529, HL83359, HL83359-S1) and Doris Duke Charitable Foundation. Dr. Krummen's work is supported by NIH grant HL83359.

Drs. Narayan and Rappel are authors of intellectual property owned by the University of California Regents and licensed to Topera Inc. Topera does not sponsor any research, including that presented here. Drs. Narayan and Rappel own equity shares in Topera. Dr. Narayan reports having received honoraria from Medtronic, St. Jude Medical, and Biotronik. Dr. Krummen has no disclosures.

Address for correspondence: Sanjiv M. Narayan, M.D., Ph.D., Professor of Medicine, University of California, San Diego, Cardiology/111A, 3350 La Jolla Village Drive, San Diego, CA 92161. Fax: 858-552-7490; E-mail: snarayan@ucsd.edu

Manuscript received 19 January 2012; Revised manuscript received 19 February 2012; Accepted for publication 5 March 2012.

doi: 10.1111/j.1540-8167.2012.02332.x

**TABLE 1**  
Clinical Characteristics

	Paroxysmal AF	Persistent AF	P
Number	19	30	
Age (years, in range)	61 ± 9 (35–77)	62 ± 9 (40–82)	0.81
History of AF (years, in range)	3.0 ± 2.6 (0.4–10.2)	6.2 ± 6.3 (0.6–28.6)	0.04
Left atrial diameter, in mm	41 ± 4	47 ± 5	0.07
LVEF, in %	59 ± 6	51 ± 13	0.30
Hypertension n (%)	16 (84)	23 (77)	0.52
Coronary disease (n, %)	7 (37)	10 (33)	0.80
Diabetes mellitus (n, %)	9 (47)	10 (33)	0.33
Medications n (%)			
ACEI/ARB	12 (63)	20 (67)	0.80
Statins	15 (79)	21 (70)	0.49
Failed antiarrhythmics			
Class I	4 (21)	7 (23)	0.85
Beta-blockers	14 (74)	22 (73)	0.98
Amiodarone	3 (16)	16 (53)	0.01
Other class III	12 (63)	14 (47)	0.26
Digoxin	5 (26)	10 (33)	0.60

LVEF = left ventricular ejection fraction.

## Methods

### Patient Flow

We recruited patients with drug-refractory AF referred for ablation for standard indications<sup>2</sup> to the Veterans Affairs and University of California Medical Centers in San Diego, on a mapping protocol approved by our joint institutional review board. Consecutive patients were approached, and all subjects provided written informed consent. The only exclusion criterion was refusal or inability to provide informed consent. These patients were used to report APD restitution,<sup>18</sup> APD alternans,<sup>19</sup> and conduction restitution<sup>20</sup> as underlying mechanisms for the dynamics of human AF. After the detailed electrophysiological mapping outlined later, all patients underwent conventional ablation for the endpoint of PV isolation.<sup>2</sup>

### Electrophysiological Mapping

Electrophysiology study was performed >5 half-lives after discontinuing antiarrhythmic medications, except for amiodarone (stopped for >30 days; Table 1). Using femoral venous access, a decapolar catheter was placed in the coronary sinus, and then a 7F monophasic action potential (MAP) catheter (Boston Scientific, Natick, MA, USA) was advanced to the right atrium then left atrium via transseptal puncture. Heparin was administered intravenously to maintain activated clotting time (ACT) >350 seconds throughout mapping (and subsequent ablation).

Simultaneous multisite recordings of the atria were achieved using 64 pole catheters (Constellation, Boston Scientific) advanced transseptally to the left atrium in all patients, with a second basket placed simultaneously in the right atrium in n = 20 patients (12 persistent, 8 paroxysmal; Fig. 1). Great care was taken to optimize electrode contact, to cover the majority of the atria and the ostia of the PVs and atrial appendages, maintaining relatively uniform inter-electrode spacing (Fig. 1). Electrodes span the orifices of the thoracic veins and atrial appendages and so this approach can identify activation emanating from, versus progressing towards, these structures.

Panels A–L of Figure 1 provide examples of optimal and suboptimal basket positions. Optimal positioning required selecting the basket size such that splines deformed slightly with cardiorespiratory motion on fluoroscopy or showed tissue opposition on intracardiac echocardiography (Fig. 1A–D). With currently available baskets (48-mm diameter, 4-mm electrode spacing; or 60-mm diameter, 5-mm electrode spacing), the LA was incompletely mapped in patients with LA diameter >≈60 mm in whom the septal LA and right PV antra were typically underrepresented (Fig. 1F).

Simultaneous biatrial basket recordings are described in this report, but the atria may also be sampled sequentially using a single basket to first analyze RA data while performing transseptal cannulation, then repeating this process for the LA.

### Electrophysiological Data Acquisition

Computational mapping was applied to native AF when possible. Patients in sinus rhythm, or in whom AF terminated before mapping, were paced into AF using a decremental protocol via cycle lengths (CLs) of 500, 450, 400, 350, and 300 milliseconds, then in 10 milliseconds steps to AF. AF was mapped after it had sustained for at least 10 minutes, because our preliminary data suggest that spatial maps of induced AF converge with maps of native AF in the same patient over this timeframe.

Multisite electrograms were recorded as unipoles (e.g., A1, A2, A3, . . .) or as overlapping bipoles (i.e., A12, A23. . .) to reduce far-field artifact, and filtered at 0.05–500 Hz. AF data were exported digitally in 1-minute epochs.

In brief, computational mapping is centrally based upon MAP data, that we used to define regional restitution of MAP duration as recently reported during pacing<sup>18,19</sup> and in AF,<sup>21</sup> and regional conduction restitution defined by conduction time to each basket electrode during progressively faster pacing to the onset of AF.<sup>20</sup>

### Nomenclature for Patient-Specific 3-Dimensional Spatiotemporal Maps of AF

Electrode positions were identified from fluoroscopy and used to identify regions of interest. Absolute electrode locations within the atria were not used for analysis but are illustrated using electroanatomic mapping with NavX (St. Jude, St. Paul, MN, USA; Fig. 2A) or CARTO (Biosense-Webster, Minneapolis, MN, USA). Figure 2B illustrates the nomenclature of 3D map projections. The left atrium was opened at its “equator” with each half of the mitral annulus reflected superiorly and inferiorly, whereas the right atrium was opened between its poles and the tricuspid annulus halves reflected laterally and septally. For illustration, Figure 2C shows sinus rhythm initiation at the high RA (red), proceeding to the LA over Bachmann’s bundle to finally activate the low lateral LA (blue), in relation to 128 biatrial electrodes (dots).

### Physiologically-Directed Computational AF Mapping

Spatiotemporal analyses of AF were performed primarily by directly analyzing electrograms to construct movies of numerous AF activation cycles (Fig. 3A), and secondarily by constructing isochronal maps to illustrate single cycle snapshots of AF (Fig. 3B). Computational mapping is a physiologically guided approach that analyses AF in the context of regional variations in the minimum tissue wavelength

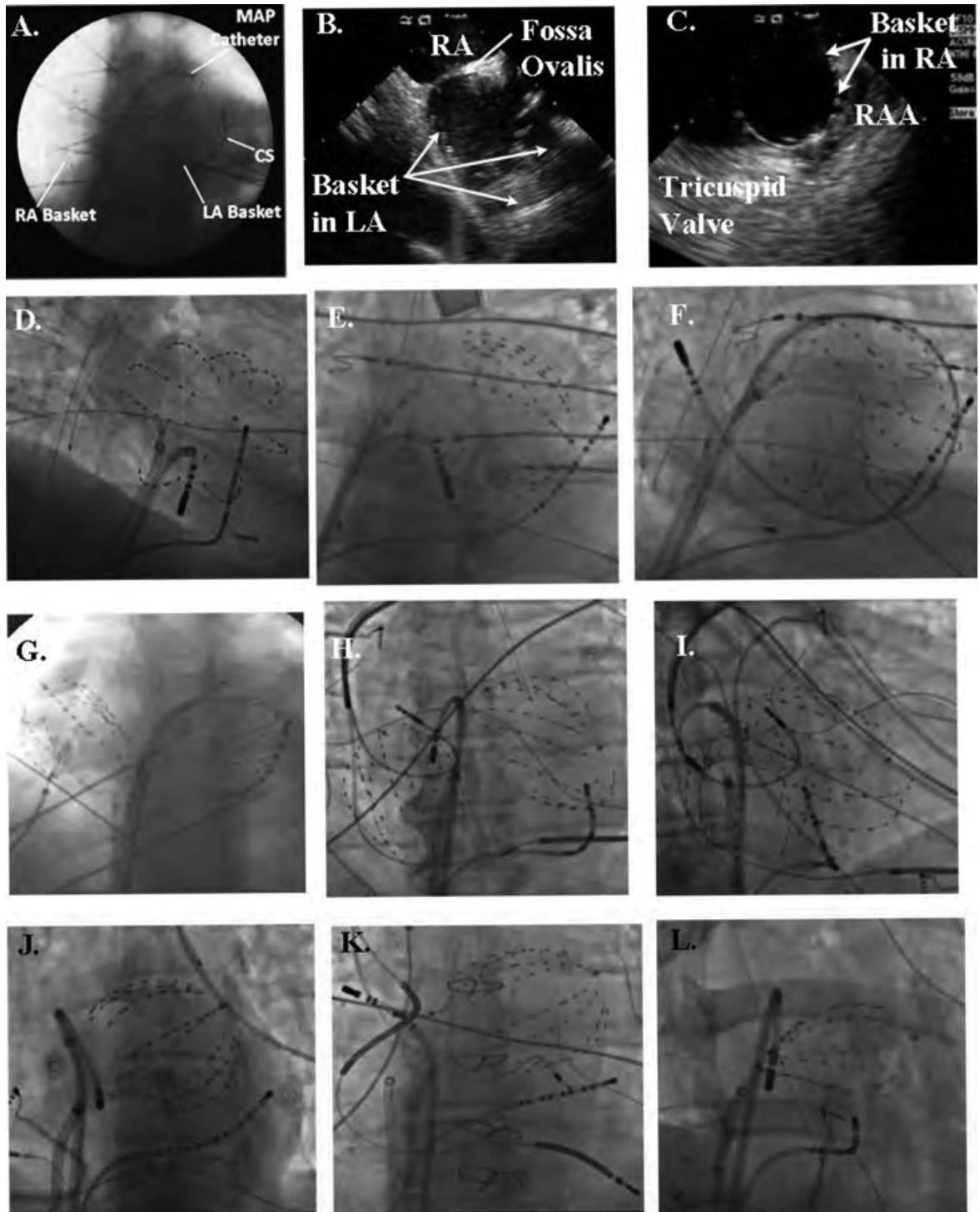


**Figure 1.** Atrial basket positioning for computational AF mapping. (A) Good catheter placement in both atria (48-mm baskets, anteroposterior fluoroscopy), with MAP catheter at the left superior pulmonary vein antrum; (B and C) intracardiac echocardiography confirms electrode opposition to walls of (B) left atrium and (C) right atrium; (D) good electrode coverage of left atrium (60-mm basket, RAO 30° fluoroscopy); (E) spline crowding detracts from otherwise good LA coverage (60-mm basket, AP fluoroscopy); (F) large left atrium, with poor electrode coverage of its septum, outlined by ablation catheter loop with tip at right superior PV ostium (60-mm basket, LAO 30° fluoroscopy); (G) poor coverage of superior LA, indicated by wide separation of LA basket from the left main bronchus; the RA basket is well deployed (60-mm baskets, AP fluoroscopy); (H) basket placement with preexisting device leads. The RA basket is well positioned in this AP projection, yet the LA basket poorly covers the inferior LA. This appearance is consistent with basket displacement through the mitral apparatus; (I) anterior displacement of the LA basket through the mitral annulus, with the ablation catheter defining the true posterior border of the LA (same patient as panel H, in 30° RAO fluoroscopy); (J) undersized basket, despite an apparently good deployment, floating freely within the large left atrium that gave very poor signals and was replaced; (K) oversized basket in a patient with heart failure, a cardiac-resynchronization defibrillator and previously diagnosed "permanent AF" now reclassified as longstanding persistent AF and undergoing ablation; (L) underexpanded basket, evident from the elliptical shape because of pinching at the interatrial septum. This was remedied by advancing the basket further into the left atrium with clockwise torque.

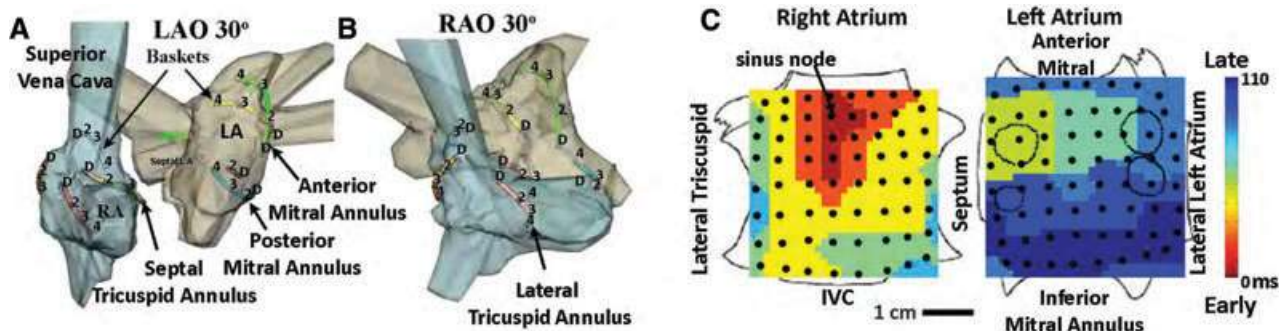


**Figure 2.** Anatomic reference and map nomenclature. (A and B) Electrodes illustrated within patient-specific atria (NavX system, St. Jude Medical, St. Paul, MN, USA) in 30° LAO and 30° RAO projections, showing alternate splines and electrodes for clarity. (C) Sinus rhythm map on biatrial schematic. Activation at basket electrodes, shown as dots, is displayed as a color-coded map from the sinus node to the lateral inferior LA. The RA is opened between its poles with tricuspid annulus opened laterally and medially; the LA is opened along its equator, with mitral annulus opened superiorly and inferiorly. The pulmonary vein ostia are indicated by dashed lines.

for reentry,  $\lambda = \text{refractory period} \times \text{conduction velocity}$ .<sup>22</sup> We used MAP recordings to define APD restitution,<sup>18,19</sup> and regional conduction restitution<sup>20</sup> to define regions of slow conduction.

In Figure 3A, movies were constructed by plotting the electrogram voltage at each electrode location at a time point T (indicated by vertical green line), then repeating this process for multiple time points to create an animation (see Supplemental movie). To circumvent the difficulty of defining CL during AF,<sup>23</sup> APD restitution defines minimum repolarization. Figure 3A illustrates a concurrent MAP tracing in AF used for this purpose. We recently reported that minimum APD and APD restitution differ markedly between patients with persistent and paroxysmal AF, yet for any one patient are consistent over time during pacing<sup>18,19</sup> or in<sup>24</sup> AF. Conduction restitution is used to define physiologically plausible propagation paths.<sup>20</sup> For instance, red and blue activation in Figure 3B lies at adjacent electrodes (4 mm apart), yet their delay ( $\approx 160$  milliseconds) could not represent direct propagation because that would require a slower than physiological CV<sup>25</sup> of 2.5 cm/s ( $= 0.4/0.16$ ).

Figure 3B illustrates an isochronal snapshot of one cycle of persistent AF indicating a counterclockwise (CCW) spiral wave (rotor, arrow) in the posterior left atrium, represented by color-coded activation from red to blue. The AF rotor indicates 1:1 activation within its proximal spiral arms, with

wavebreak and collision (fibrillatory conduction) at the spiral arm periphery and beyond.

### Definition of Localized Sources

Computational maps were analyzed to reveal sustained localized sources of human AF in the form of focal impulse<sup>15,26</sup> or rotor<sup>6</sup> maps (FIRM) as shown in animal models but not previously in human AF.<sup>6,27</sup> Rotors were identified as rotational activity around a center (using isopotential movies and isochronal activation maps). Focal beats in AF were identified at their point of origin from surrounding diastole from isopotential movies and isochronal maps. We diagnosed rotors or focal beat sources only if sustained throughout several recording epochs (arbitrarily  $>50$  cycles), to exclude transient rotational and/or centrifugal activation that by definition cannot represent sources but likely represent wavebreak and/or passive activation that are highly variable in fibrillation.

### Statistical Analysis

Continuous data are represented as mean  $\pm$  standard deviation (SD). The *t*-test was used to compare variables between 2 groups, such as LA area or AF CL. Paired continuous variables were compared using linear regression and the paired *t*-test. The chi-square test was applied to contingency

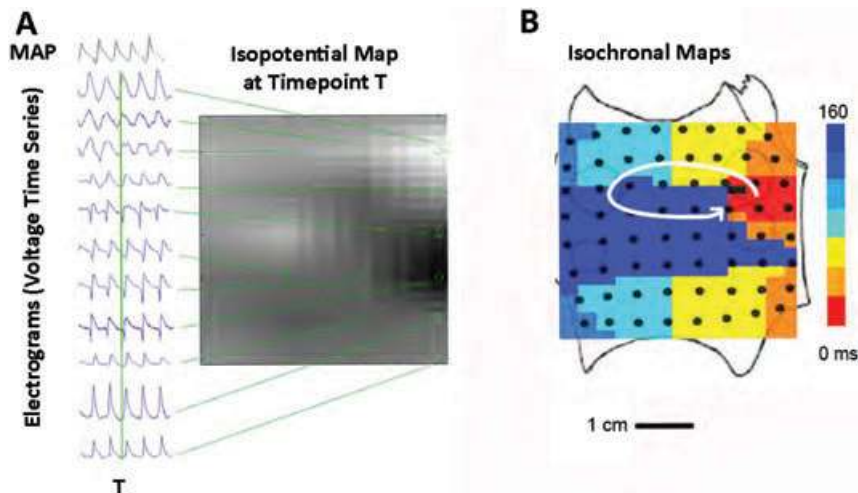


**Figure 3.** Mapping reveals spiral wave during AF in the human left atrium. (A) Raw electrograms used to create maps and movies. Unipolar electrograms (locations indicated by circles on grid) are used to construct an isopotential snapshot at any time point T (indicated by vertical green line). Monophasic action potentials (MAP) indicate repolarization and are used to calibrate unipolar electrograms. These isopotential maps are created successively for multiple time points T to create movies (see Supplemental movie). (B) Isochronal snapshot of an LA rotor during one cycle of AF, created from activation times determined when each unipolar electrogram crosses a voltage threshold.

**TABLE 2**  
Characteristics of Localized AF Sources

Characteristic	Paroxysmal AF (n = 19)	Persistent AF (n = 30)	P
AF CL, in milliseconds	187 ± 25	163 ± 19	<0.001
Number of patients with sources	19 (100%)	28 (94%)	–
Number of sources/Pt (biatrial cases)	1.5 ± 0.8	2.1 ± 1.0	0.017
Number of rotors/focal beats (biatrial)	16/6	41/5	0.09
LA recordings, n	19	30	–
Rotors/focal beats (LA), n	12/4	29/4	–
RA recordings, n	8	12	–
Rotors/focal beats (RA), n	4/2	12/1	–

tables. A probability of <5% was considered statistically significant.

**Results**

Table 1 indicates the clinical characteristics of our population.

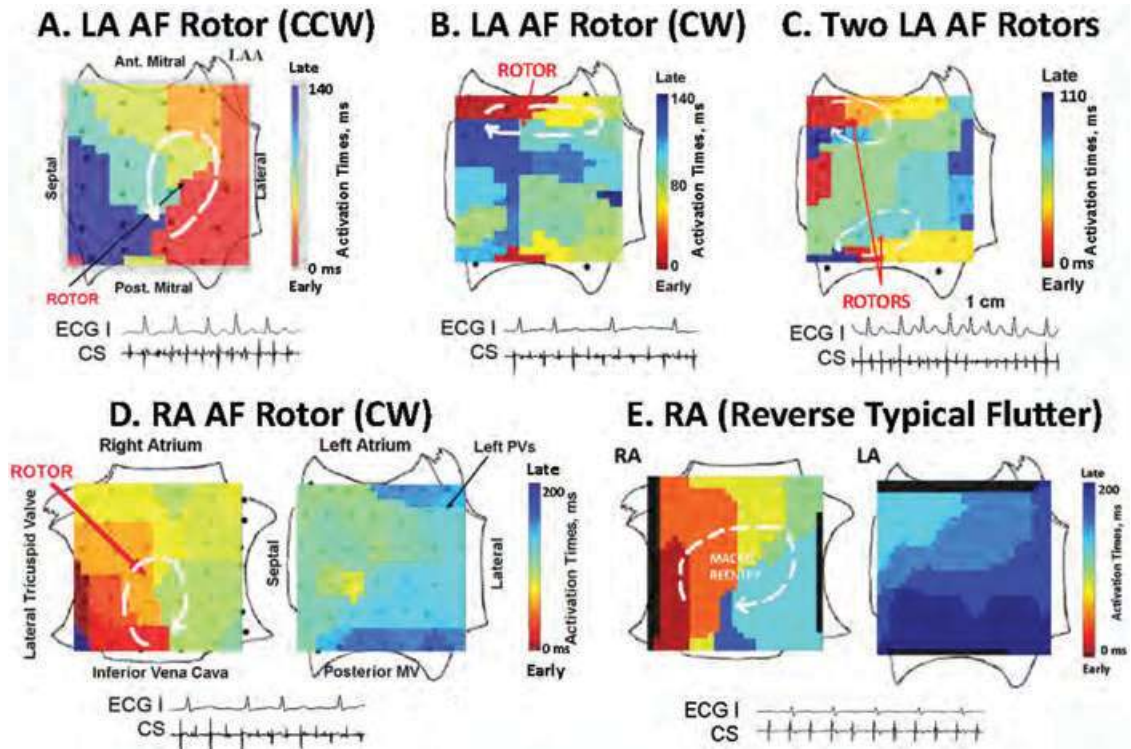
**Computational Mapping of Electrical Rotors During Human AF**

Computational mapping revealed electrical rotors or focal beats during AF in 47 of 49 (95.9%) patients (Table 1), that were sustained throughout multiple epochs over many min-

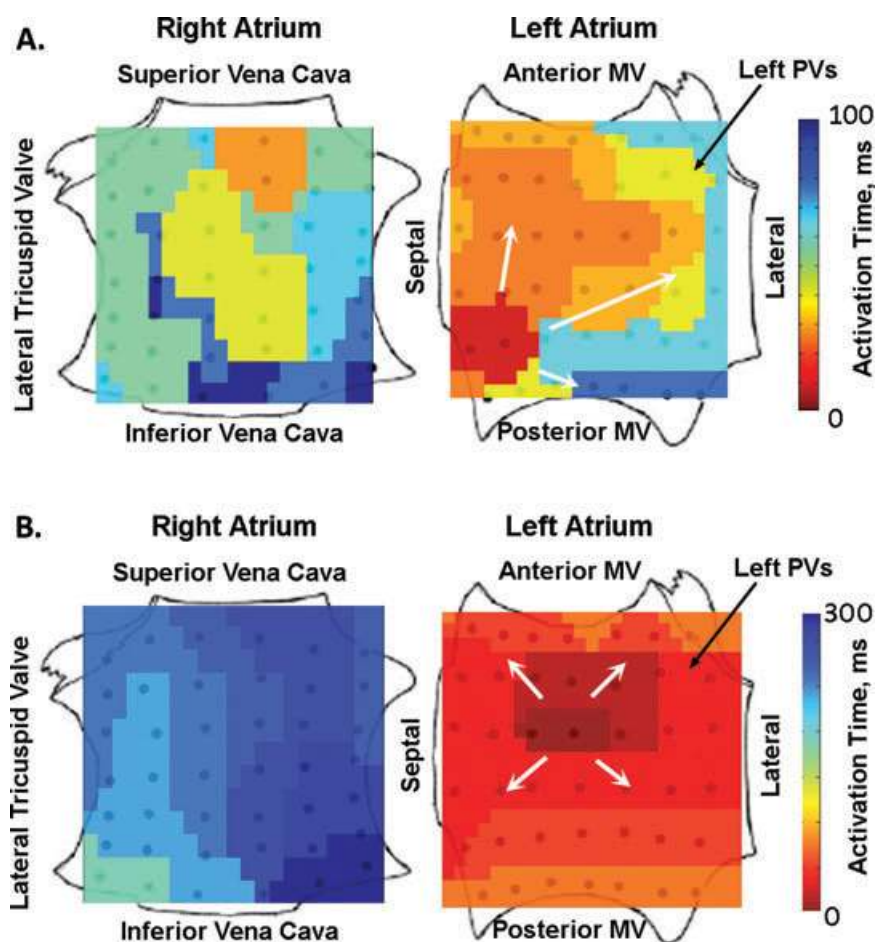
utes (i.e., thousands of cycles). These regions exhibited 1:1 activation of atrial activation within their spiral arms, with propagation to the remaining atria characterized by wave-break or “fibrillatory conduction” (disorganization of 1:1 activation) distally and in the contralateral atrium. Thus, rotors and focal beats were sources for AF activation rather than passively activated elements.

Figure 4A (50-year-old man with persistent AF and LA diameter 52 mm) shows a solitary rotor in the mid-posterior LA during AF with CCW activation represented by the red-to-blue color coded activation with CL 140 milliseconds. This rotor accounted for 1:1 activation in ≈70% of the LA (its spiral arms), with fibrillatory conduction shown by collision between late activation from the rotor in the inferoposterior wall (blue) with early activation from asynchronous activation at the inferior mitral annulus (red/yellow) and to the coronary sinus (see electrograms). Figure 4B illustrates a clockwise (CW) rotor that controls a smaller region of the atrium during persistent AF in the anterior LA in a 62-year old with LA diameter 52 mm and heart failure (left ventricular ejection fraction [LVEF] 37%).

Table 2 summarizes that most patients had multiple concurrent sources, typically in the left and right atrium. Figure 4C shows 2 concurrent rotors in the left atrium during paroxysmal AF in the anterior LA (CW) and inferior LA (CCW). Figure 4D shows biatrial maps illustrating a CW rotor in the mid-posterior RA during paroxysmal AF, with fibrillatory conduction to the LA in a 66-year-old Native American with LA diameter of 42 mm.



**Figure 4.** Localized electrical rotors (spiral waves) in human AF, revealed by computational mapping. (A) Solitary counterclockwise (CCW) rotor during persistent AF in the posterior LA; (B) CW rotor in persistent AF in the anterior LA; (C) 2 concurrent rotors during paroxysmal AF in the anterior LA (CW) and inferior LA (CCW); (D) right atrial rotor (CW) during paroxysmal AF in the mid-posterior wall, with fibrillatory conduction to the LA. By contrast, (E) clockwise rotor of reverse typical atrial flutter differs from AF, with 1:1 activation throughout the RA that engages Bachmann’s bundle to activate the LA and no fibrillatory conduction. Key: ECG lead I. CS = coronary sinus electrogram.



**Figure 5.** Repetitive focal beats revealed by computational mapping. (A) Repetitive focal beat during paroxysmal AF (in low septal LA), with activation to remaining LA and fibrillatory conduction to the RA (CL  $\approx$  100 milliseconds). In contrast, (B) focal atrial tachycardia (nonfibrillatory) from the high posterior LA differs from AF by showing 1:1 activation centrifugally to the ipsilateral then contralateral atria (CL  $\approx$  300 milliseconds).

Although some AF rotors appeared relatively organized in single isochronal snapshots, static images do not reflect rotor precession (limited movement) seen in multicycle animations (Supplemental Movie) and may not emphasize peripheral breakdown of 1:1 conduction. In contrast, Figure 4E illustrates true 1:1 biatrial activation (with no fibrillatory conduction) from CW macroreentry in the right atrium (reverse typical atrial flutter) and activation to the left atrium over Bachmann's bundle.

#### Demonstration of Focal Beats During Human AF

Repetitive focal beats were visualized represented 11 of 68 (16.2%) of sources in patients during paroxysmal and persistent AF (Table 2). The FIRM map of AF in Figure 5A shows earliest biatrial activation emanating from a repetitive focal beat (CL 104 milliseconds) in the inferoseptal LA in a 67-year-old man with persistent AF, moderately dilated LA and left ventricular ejection fraction 45%. Notably, activation emanates radially but nonuniformly to surrounding LA (arrows), with wavebreak in the peripheral LA then contralateral RA. In contrast, Figure 5B shows a FIRM map of focal atrial tachycardia (CL 290 milliseconds) located in the mid-posterior LA, with organized and uniform centrifugal activation throughout the ipsilateral LA to the contralateral RA.

#### Localized Sources Were Prevalent in Human AF

Computational mapping revealed localized sources in nearly all patients, with most exhibiting multiple sources

(Table 2). The number of concurrent AF sources was higher for patients with persistent than paroxysmal AF ( $P = 0.017$ ; Table 2) and, surprisingly, 27% lay in the right atrium. The number of rotors was greater than the number of focal beats, and this ratio trended higher for patients with persistent AF (41:5) than paroxysmal AF (16:6;  $P = 0.088$ ).

There were no complications during mapping.

#### Discussion

We report a novel physiological mapping approach for human AF that reveals, for the first time, sustained localized electrical rotors and repetitive focal beat sources for human AF. We identified localized sources in nearly all AF patients, who had an average of 1.5–2 sources that directly controlled local activation with breakdown of 1:1 conduction (wavebreak, or “fibrillatory conduction”) to surrounding regions. Persistent AF exhibited a higher number of concurrent rotors or focal beat sources than paroxysmal AF, and that may explain the greater apparent complexity and difficulty of treatment of this AF phenotype. These findings shed novel insights into the mechanisms of human AF, and provide the foundation for a patient-tailored mechanistic approach to AF ablation.

#### Computational Mapping Compared to Prior Mapping of Human AF

This study reveals that human AF is predominantly caused by localized sources that control surrounding fibrillation and,

for each patient, lie at patient-specific locations that remain stable for at least tens of minutes (thousands of cycles). Although localized AF sources have been shown in elegant animal models in the laboratories of Jalife<sup>6,28</sup> and Waldo,<sup>15,29</sup> recent human studies have reported that rotors are rare<sup>16</sup> or do not exist<sup>8,27,30</sup> in human AF. Methodologic differences may explain our divergence from those data.

Allessie *et al.*, in pioneering human AF mapping, initially showed complex right atrial activation consistent with multiple wavelets during electrically induced AF in patients undergoing open-chest ablation for accessory pathways.<sup>8,30</sup> Those findings were recently extended to the left atrium and persistent AF patients.<sup>27</sup> However, although those studies provide high spatial resolution, they sampled relatively narrow and fixed areas using plaques in the anterolateral right atrium and posterior left atrium, where sources may not exist in all patients. In contrast, wide-area mapping in computational mapping makes no assumptions about the spatial uniformity of human AF. The spatial resolution of baskets (4–5-mm interelectrode distance along a spline) provides sufficient spatial resolution to resolve small human reentry circuits ( $\approx 2 \text{ cm}^2$ ),<sup>22</sup> although regions that as sources (reentrant or focal) should be detectable at a greater distance.<sup>31</sup> Finally, if ablation is the clinical goal, then higher resolution may be moot given that the diameter of a single ablation lesion is  $\approx 7 \text{ mm}$ . Computational mapping also benefited from our recent studies documenting, for the first time, differences in human biatrial repolarization and conduction dynamics from animal studies, and between patients with paroxysmal and persistent AF.<sup>18,19</sup>

Notably, other studies provide indirect evidence for the existence of localized sources in human AF. Sahadevan *et al.* reported  $n = 9$  patients with persistent AF at open-chest surgery, in whom gradients of rate, organization, and spectral dominant frequency (DF)<sup>11</sup> were consistent with localized sources, although spatial AF activation maps were not created and interventions were not performed. Using non-contact maps, Lin *et al.* revealed regions of high dominant frequency during macroreentry and imminent disorganization to AF.<sup>32</sup> We recently used LA baskets to show gradients in spectral DF and organization at specific sites, of which some corresponded to sites of AF termination during extensive ablation.<sup>33</sup> Studies using lower resolution mapping also confirm consistent gradients in rate, consistent with regional “driver regions,” during human AF.<sup>10,34</sup> In addition, Ravelli *et al.* used RA baskets to show consistent sites of electrogram organization in human AF.<sup>35</sup> Unlike the present report, however, prior reports did not reveal rotors or repetitive focal beat sources, did not identify nor locate AF sources, nor did they demonstrate using activation mapping that any specific region determines activation in surrounding tissue during human AF.

### Clinical Implications

These mechanistic findings provide potential insights into the results of AF ablation. The greater number of sources in patients with persistent versus paroxysmal AF is consistent with more difficult ablation in the former group. Patient-specific source locations may explain why extensive ablation outside of the PVs is often required to eliminate AF.<sup>2</sup> The presence of right atrial sources in one-quarter of patients may explain the 70–80% “ceiling” in AF ablation success in

many current studies, even after 3 or more (predominantly left atrial) procedures.<sup>2</sup> Future studies should apply computational mapping prospectively and target electrical rotors and focal beats for ablation or other therapeutic modalities, such as pharmaceutical or regenerative therapy, to terminate and eliminate AF. Other applications of computational mapping are to track patient-specific AF mechanisms longitudinally over time, to assess the progression of atrial remodeling or possible reverse remodeling from antiarrhythmic medications, gene therapy, stem cell therapy, or pacing.

### Limitations

In this series, ablation was not performed prospectively at localized sources because early iterations of computational mapping required hours to days of processing time. Prospective mapping studies with targeted ablation of sources, that is, FIRM are underway. Although the population is relatively small, it represents a typical tertiary care referral group including patients with and without heart failure, of young and advanced age, with short to very long AF durations, and normal-sized to very enlarged atria. Thus, we feel that our description of rotors and focal beat sources is robust and likely applies to the vast majority of patients referred for AF ablation. Patients with persistent AF had a higher historical usage of amiodarone than those with paroxysmal AF, but the drug was discontinued  $>60$  days before the procedure in all cases (often more than a year before enrollment). Although epicardial and endocardial signals may differ in regions of thick atrial musculature,<sup>9</sup> we did not perform epicardial mapping in this series. We did not exhaustively analyze regions of complex fractionated atrial electrograms in the present report, and also did not evaluate the impact of autonomic function on localized sources. Patients in this series were predominantly male, but more recent studies have already extended these observations to women. As shown in Figure 1, technical factors such as LA diameter  $>60 \text{ mm}$  may prevent adequate mapping in patients with very advanced structural remodeling, although this may be mitigated if larger baskets become available.

### Conclusions

Physiologically guided computational mapping revealed localized electrical rotors and repetitive focal beat sources for human AF for the first time. The vast majority of AF patients showed localized sources, for an average of 1.5–2 concurrent rotors and/or focal beats, that controlled local AF activation and caused peripheral wavebreak. One-quarter lay in the right atrium. These results shed novel mechanistic insights into human AF, and offer a foundation for mechanistically targeted patient-tailored approaches to AF ablation.

### References

- Haissaguerre M, Jais P, Shah DC, Takahashi A, Hocini M, Quiniou G, Garrigue S, Le Mouroux A, Le Metayer P, Clementy J: Spontaneous initiation of atrial fibrillation by ectopic beats originating in the pulmonary veins. *N Engl J Med* 1998;339:659-666.
- Calkins H, Kuck KH, Cappato R, Brugada J, Camm AJ, Chen SA, Crijns HJ, Damiano RJ Jr, Davies DW, Dimarco J, Edgerton J, Ellenbogen K, Ezekowitz MD, Haines DE, Haissaguerre M, Hindricks G, Iesaka Y, Jackman W, Jalife J, Jais P, Kalman J, Keane D, Kim YH, Kirchhof P, Klein G, Kottkamp H, Kumagai K, Lindsay BD, Mansour M, Marchlinski FE, McCarthy PM, Mont JL, Morady F,

- Nademanee K, Nakagawa H, Natale A, Nattel S, Packer DL, Pappone C, Prystowsky E, Raviele A, Reddy V, Ruskin JN, Shemin RJ, Tsao HM, Wilber D: 2012 HRS/EHRA/ECAS expert consensus statement on catheter and surgical ablation of atrial fibrillation: Recommendations for patient selection, procedural techniques, patient management and follow-up, definitions, endpoints, and research trial design. *Heart Rhythm* 2012;9:632-696.e21.
3. Weimar T, Bailey MS, Watanabe Y, Marin D, Maniar HS, Schuessler RB, Damiano RJ Jr: The Cox-maze IV procedure for lone atrial fibrillation: A single center experience in 100 consecutive patients. *J Interv Card Electrophysiol* 2011;31:47-54
  4. Weerasooriya R, Khairy P, Litalien J, Macle L, Hocini M, Sacher F, Lellouche N, Knecht S, Wright M, Nault I, Miyazaki S, Scavee C, Clementy J, Haissaguerre M, Jais P: Catheter ablation for atrial fibrillation: Are results maintained at 5 years of follow-up? *J Am Coll Cardiol* 2011;57:160-166.
  5. Nattel S: New ideas about atrial fibrillation 50 years on. *Nature* 2002;415:219-226.
  6. Vaquero M, Calvo D, Jalife J: Cardiac fibrillation: From ion channels to rotors in the human heart. *Heart Rhythm* 2008;5:872-879.
  7. Zipes DP, Jalife J: *Cardiac Electrophysiology: From Cell to Bedside*. Saunders, Elsevier: London, 2009.
  8. Konings K, Kirchhof C, Smeets J, Wellens H, Penn O, Allessie M: High-density mapping of electrically induced atrial fibrillation in humans. *Circulation* 1994;89:1665-1680.
  9. Allessie MA, de Groot NM, Houben RP, Schotten U, Boersma E, Smeets JL, Crijns HJ: The electropathological substrate of longstanding persistent atrial fibrillation in patients with structural heart disease: Longitudinal dissociation. *Circ Arrhythm Electrophysiol* 2010;3:606-615.
  10. Lazar S, Dixit S, Marchlinski FE, Callans DJ, Gerstenfeld EP: Presence of left-to-right atrial frequency gradient in paroxysmal but not persistent atrial fibrillation in humans. *Circulation* 2004;110:3181-3186.
  11. Sahadevan J, Ryu K, Peltz L, Khrestian CM, Stewart RW, Markowitz AH, Waldo AL: Epicardial mapping of chronic atrial fibrillation in patients: Preliminary observations. *Circulation* 2004;110:3293-3299.
  12. Beukema WP, Sie HT, Misier AR, Delnoy PP, Wellens HJ, Elvan A: Predictive factors of sustained sinus rhythm and recurrent atrial fibrillation after a radiofrequency modified Maze procedure. *Eur J Cardiothorac Surg* 2008;34:771-775.
  13. Davidenko JM, Pertsov AV, Salomonsz R, Baxter W, Jalife J: Stationary and drifting spiral waves of excitation in isolated cardiac muscle. *Nature* 1992;355:349-351.
  14. Ideker RE, Rogers JM: Human ventricular fibrillation: Wandering wavelets, mother rotors, or both? *Circulation* 2006;114:530-532.
  15. Ryu K, Shroff SC, Sahadevan J, Martovitz NL, Khrestian CM, Stambler BS: Mapping of atrial activation during sustained atrial fibrillation in dogs with rapid ventricular pacing induced heart failure: Evidence for a role of driver regions. *J Cardiovasc Electrophysiol* 2005;16:1348-1358.
  16. Cuculich PS, Wang Y, Lindsay BD, Faddis MN, Schuessler RB, Damiano RJ Jr, Li L, Rudy Y: Noninvasive characterization of epicardial activation in humans with diverse atrial fibrillation patterns. *Circulation* 2010;122:1364-1372.
  17. Atenza F, Calvo D, Almendral J, Zlochiver S, Grzeda KR, Martinez-Alzamora N, Gonzalez-Torrecilla E, Arenal A, Fernandez-Aviles F, Berenfeld O: Mechanisms of fractionated electrograms formation in the posterior left atrium during paroxysmal atrial fibrillation in humans. *J Am Coll Cardiol* 2011;57:1081-1092.
  18. Narayan SM, Kazi D, Krummen DE, Rappel W-J: Repolarization and activation restitution near human pulmonary veins and atrial fibrillation initiation: A mechanism for the initiation of atrial fibrillation by premature beats. *J Am Coll Cardiol* 2008;52:1222-1230.
  19. Narayan SM, Franz MR, Clopton P, Pruvot EJ, Krummen DE: Repolarization alternans reveals vulnerability to human atrial fibrillation. *Circulation* 2011;123:2922-2930.
  20. Lalani G, Schricke A, Gibson M, Rostamian A, Krummen DE, Narayan SM: Dynamic conduction slowing precedes human atrial fibrillation initiation: Insights from bi-atrial basket mapping on transitions to atrial fibrillation. *J Am Coll Cardiol* 2012;59:595-606.
  21. Narayan SM, Franz MR: Quantifying fractionation and rate in human atrial fibrillation using monophasic action potentials: Implications for substrate mapping. *Europace* 2007e;9:vi89-vi95.
  22. Rensma P, Allessie M, Lammers W, Bonke F, Schalij M: Length of excitation wave and susceptibility to reentrant atrial arrhythmias in normal conscious dogs. *Circ Res* 1988;62:395-410.
  23. Elvan A, Linnenbank A, van Bommel M, Misier A, Delnoy P, Beukema WP, de Bakker J: Dominant frequency of atrial fibrillation correlates poorly with atrial fibrillation cycle length. *Circ Arrhythm Electrophysiol* 2009;2:634-644.
  24. Narayan SM, Krummen DE, Kahn AM, Karasik PL, Franz MR: Evaluating Fluctuations in human atrial fibrillatory cycle length using monophasic action potentials. *Pacing Clin Electrophysiol* 2006;29:1209-1218.
  25. Harrild DM, Henriquez CS: A computer model of normal conduction in the human atria. *Circ Res* 2000;87:e25-e36.
  26. Yamazaki M, Vaquero LM, Hou L, Campbell K, Zlochiver S, Klos M, Mironov S, Berenfeld O, Honjo H, Kodama I, Jalife J, Kalifa J: Mechanisms of stretch-induced atrial fibrillation in the presence and the absence of adrenergic stimulation: Interplay between rotors and focal discharges. *Heart Rhythm* 2009;6:1009-1017.
  27. de Groot NM, Houben RP, Smeets JL, Boersma E, Schotten U, Schalij MJ, Crijns H, Allessie MA: Electropathological substrate of long-standing persistent atrial fibrillation in patients with structural heart disease: Epicardial breakthrough. *Circulation* 2010;122:1674-1682.
  28. Skanes AC, Mandapati R, Berenfeld O, Davidenko JM, Jalife J: Spatiotemporal periodicity during atrial fibrillation in the isolated sheep heart. *Circulation* 1998;98:1236-1248.
  29. Waldo AL, Feld GK: Inter-relationships of atrial fibrillation and atrial flutter mechanisms and clinical implications. *J Am Coll Cardiol* 2008;51:779-786.
  30. Konings K, Smeets J, Penn O, Wellens H, Allessie M: Configuration of unipolar atrial electrograms during electrically induced atrial fibrillation in humans. *Circulation* 1997;95:1231-1241.
  31. Ideker RE, Rogers JM, Fast V, Li L, Kay GN, Pogwizd SM: Can mapping differentiate microreentry from a focus in the ventricle? *Heart Rhythm* 2009;6:1666-1669.
  32. Lin YJ, Tai CT, Kao T, Tso HW, Huang JL, Higa S, Yuniadi Y, Huang BH, Liu TY, Lee PC, Hsieh MH, Chen SA: Electrophysiological characteristics and catheter ablation in patients with paroxysmal right atrial fibrillation. *Circulation* 2005;112:1692-1700.
  33. Krummen DE, Peng KA, Bullinga JR, Narayan SM: Centrifugal gradients of rate and organization in human atrial fibrillation. *Pacing Clin Electrophysiol* 2009;32:1366-1378.
  34. Lemola K, Ting M, Gupta P, Anker JN, Chugh A, Good E, Reich S, Tschopp D, Igic P, Elmouchi D, Jongnarangsin K, Bogun F, Pelosi F, Morady F, Oral H: Effects of two different catheter ablation techniques on spectral characteristics of atrial fibrillation. *J Am Coll Cardiol* 2006;48:340-348.
  35. Ravelli F, Faes L, Sandrini L, Gaita F, Antolini R, Scaglione M, Nollo G: Wave similarity mapping shows the spatiotemporal distribution of fibrillatory wave complexity in the human right atrium during paroxysmal and chronic atrial fibrillation. *J Cardiovasc Electrophysiol* 2005;16:1071-1076.

### Supporting Information

Additional Supporting Information may be found in the online version of this article:

**Supplemental Movie.** Shows several cycles of AF maps in this case, with electrical activation coded on a gray scale with white corresponding to activated tissue and black corresponding to recovered tissue. The white dots correspond to potential rotor sites, with the only sustained rotor indicated by the white dot at the top of the movie (anterior left atrium).

**Supplemental Figure.** Shows a left atrial rotor in the anterior left atrium during persistent AF in a 52-year-old man with left ventricular ejection fraction of 37% and left atrial diameter of 52 mm. Activation is color coded for one cycle from red (early) to blue (late) for an AF cycle length of approximately 150 milliseconds. Anatomic orientation of the left atrium is labeled.

Please note: Wiley-Blackwell is not responsible for the content or functionality of any supporting materials supplied by the authors. Any queries (other than missing material) should be directed to the corresponding author for the article.